Interactions between Heme *d* and Heme b_{595} in Quinol Oxidase *bd* from *Escherichia coli:* A Photoselection Study Using Femtosecond Spectroscopy†

Vitaliy B. Borisov,‡ Ursula Liebl,§ Fabrice Rappaport,|| Jean-Louis Martin,§ Jie Zhang,⊥ Robert B. Gennis,⊥ Alexander A. Konstantinov,‡ and Marten H. Vos*,§

A. N. Belozersky Institute of Physico-Chemical Biology, Moscow State University, Moscow 119899, Russia, Laboratory for Optical Biosciences, INSERM U451, CNRS UMR 7645, Ecole Polytechnique-ENSTA, 91128 Palaiseau Cedex, France, Institut de Biologie Physico-Chimique, CNRS UPR 1261, 13 rue Pierre et Marie Curie, 75005 Paris, France, and Department of Biochemistry, University of Illinois at Urbana−Champaign, 600 South Mathews Street, Urbana, Illinois 60801

Received September 25, 2001; Revised Manuscript Received November 22, 2001

ABSTRACT: Femtosecond spectroscopy was performed on CO-liganded (fully reduced and mixed-valence states) and O_2-liganded quinol oxidase *bd* from *Escherichia coli*. Substantial polarization effects, unprecedented for optical studies of heme proteins, were observed in the CO photodissociation spectra, implying interactions between heme *d* (the chlorin ligand binding site) and the close-lying heme b_{595} on the picosecond time scale; this general result is fully consistent with previous work [Vos, M. H., Borisov, V. B., Liebl, U., Martin, J.-L., and Konstantinov, A. A. (2000) *Proc. Natl. Acad. Sci. U.S.A. 97*, 1554−1559]. Analysis of the data obtained under isotropic and anisotropic polarization conditions and additional flash photolysis nanosecond experiments on a mutant of cytochrome *bd* mostly lacking heme b_{595} allow to attribute the features in the well-known but unusual CO dissociation spectrum of cytochrome *bd* to individual heme *d* and heme b_{595} transitions. This renders it possible to compare the spectra of CO dissociation from reduced and mixed-valence cytochrome *bd* under static conditions and on a picosecond time scale in much more detail than previously possible. CO binding/dissociation from heme *d* is shown to perturb ferrous heme b_{595}, causing induction/loss of an absorption band centered at ∼435 nm. In addition, the CO photodissociation-induced absorption changes at 50 ps reveal a bathochromic shift of ferrous heme b_{595} relative to the static spectrum. No evidence for transient binding of CO to heme b_{595} after dissociation from heme *d* is found in the picosecond time range. The yield of CO photodissociation from heme *d* on a time scale of <15 ps is found to be diminished more than 3-fold when heme b_{595} is oxidized rather than reduced. In contrast to other known heme proteins, molecular oxygen cannot be photodissociated from the mixed-valence cytochrome *bd* at all, indicating a unique structural and electronic configuration of the diheme active site in the enzyme.

Quinol oxidases of the *bd* type constitute a class of terminal respiratory oxidases widely spread in prokaryotes that are responsible for the so-called "cyanide-insensitive respiration" (*1*) and allow bacteria to survive under low oxygen pressure conditions due to their high affinity for molecular oxygen and turnover rates approaching diffusion limit (reviewed in refs *2*−*4*). There is growing evidence that cytochrome *bd* expression is a prerequisite for the virulence of many pathogenic bacteria, such as *Brucella abortus* (*5*), *Shigella* spp. (bacillary disentery) (*6*), and *Salmonella typhimurium* (*7*).

Cytochromes *bd* form their own gene sequence phylogenetic tree (*8*) but do not show sequence homology with other proteins, including the family of the functionally similar heme−copper oxidases that catalyze the same chemical reaction of dioxygen reduction to water but differ from *bd* oxidases in both structure and mechanism. The heme−copper oxidases contain hemes and copper ions as redox-active centers, and the dioxygen reduction is catalyzed by a binuclear site comprised of a high-spin heme (e.g., heme a_3) and a nearby copper ion called Cu_B (*9*). In contrast, *bd*-type oxidases do not contain copper, only hemes (three per enzyme molecule). Interestingly, close to the high-spin heme *d*, which is a functional analogue of heme a_3 in cytochrome *c* oxidase and binds dioxygen and other low molecular weight exogenous ligands, there is a second iron−porphyrin group, high-spin heme b_{595}, that interacts with heme *d* and affects the dynamics and pathways of ligand binding with the latter (*10*−*14*). Therefore, reduction of dioxygen to water in *bd*-type oxidases may be regarded to take place in a diheme, as opposed to the heme−copper, binuclear site. In addition, the

† Supported by a PECO grant from INSERM, Grants 99-04-48095 (V.B.B.) and 00-04-48251 (A.A.K.) from the Russian Fund for Basic Research, Howard Hughes Medical Institute International Scholar Award 55000320 (A.A.K.), Grant HL16101 from the National Institutes of Health (R.B.G.), and Fellowship Grant for Young Scientists 01/1-0015 from the International Association for the promotion of cooperation with scientists from the New Independent States of the former Soviet Union (V.B.B.). V.B.B.'s visit to the Institut de Biologie Physico-Chimique CNRS was supported by a FEBS short-term fellowship.

* Corresponding author. Phone: 33 1 69334777. Fax: 33 1 69333017. E-mail: Marten.Vos@polytechnique.fr.

‡ Moscow State University.

§ Laboratory for Optical Biosciences.

|| Institut de Biologie Physico-Chimique.

⊥ University of Illinois at Urbana−Champaign.

10.1021/bi0158019 CCC: $22.00
Published on Web 01/09/2002

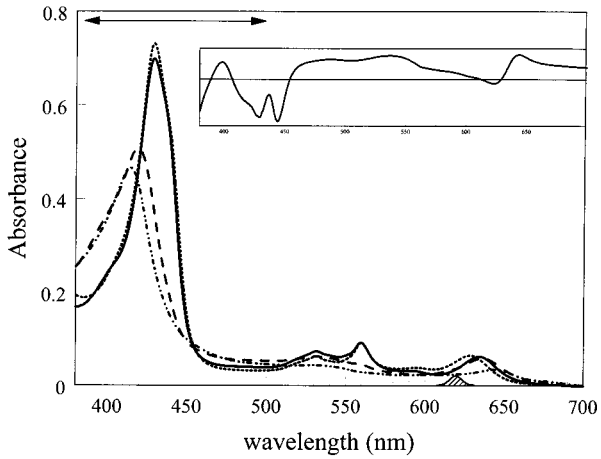

FIGURE 1: Steady-state absorption spectra of the reduced unliganded (R, dotted), reduced−CO (R−CO, solid), mixed valence−CO (MV−CO, dashed), and as-prepared (MV−O_2, dash−dot) complexes. The spectral profile of the pump pulse and the probe region in the transient absorption experiments are indicated by the shaded area at the bottom and the bisided arrow, respectively. Inset: absorption changes induced by low CO concentrations: difference between reduced 20 μM CO-equilibrated and unliganded form (enzyme concentration 10 μM).

bd complex contains a third heme b_{558} that is low spin and serves to shuttle the electrons from the quinol substrate to the dioxygen reduction site. In contrast to the majority of heme−copper oxidases, the cytochrome *bd* complex does not pump protons (*15*), although it supports charge separation across the bacterial membrane (cf. ref *16* and references cited therein). Whereas a 3D structure has been published for several heme−copper cytochrome *c* oxidases (*17*−*19*), no crystal structure is available yet for the cytochrome *bd* family, and the molecular mechanism of the enzyme action has been studied in much less detail than that of heme−copper oxidases. In particular, the molecular origin of its high affinity for oxygen is not well understood.

The proposed proxicity and interplay between the two different porphyrin cofactors ("heme" *d* contains an unsaturated pyrrole ring and is therefore formally a chlorin) make it particularly amenable for optical spectroscopic studies. Using femtosecond spectroscopy under the conditions of selective excitation of the hemes, we have recently demonstrated (*14*) that the unusual shape of the ligand (CO) dissociation spectrum of the fully reduced enzyme (Figure 1) originates from the interaction between the two hemes and that the redox state of heme b_{595} influences this interaction [the latter heme itself is hardly capable of CO binding (*20*, *21*)]. As noted in ref *14*, a detailed interpretation of the time-resolved spectra may be complicated by photoselection (polarization) effects that normally do not interfere with ultrafast heme protein studies, where different hemes can be regarded as "independent" on the time scale of the experiment. In the present work, we have performed femto/picosecond studies of CO photodissociation from cytochrome *bd* under conditions where photoselection does not play a role, which allows for a detailed comparison between the photoinduced absorption changes at different redox states. In addition, we have studied the photoselection effects in detail and exploited the unusual features found to obtain information about the heme−heme and heme−CO interactions. This information has been compared to preliminary results of nanosecond spectroscopy on membranes containing a mutant mostly lacking heme b_{595} (*22*). Finally, comparative studies with O_2 as a ligand reveal a unique photostability of the oxy complex of heme d^{2+} and suggest that the diheme character of the active site plays a role in the high oxygen affinity of cytochrome *bd*.

MATERIALS AND METHODS

Wild-type (WT) cytochrome *bd* from *Escherichia coli* was isolated as described previously (*14*). Measurements were made at room temperature in a buffer containing 50 mM Hepes, 50 mM Ches (pH 8), 0.5 mM EDTA, and 0.025% sodium *N*-lauroylsarcosinate in a 1 mm optical pathway cell at an enzyme concentration of 21 μM. The as-prepared (MV−O_2,[1] predominantly $b_{558}^{3+}b_{595}^{3+}d^{2+}$−$O_2$**)** enzyme, the fully reduced (50 mM dithionite) unliganded state (R, $b_{558}^{2+}b_{595}^{2+}d^{2+}$), the carbon monoxide complex of the fully reduced state (R−CO, $b_{558}^{2+}b_{595}^{2+}d^{2+}$−CO), and the carbon monoxide complex of the mixed-valence state (MV−CO, $b_{558}^{3+}b_{595}^{3+}d^{2+}$−CO) were obtained as described (*14*). Unless indicated otherwise, the results refer to these preparations.

Membranes from the wild-type and mutant (E445A) cells of *E. coli* used in the nanosecond CO photodissociation experiments were prepared in Urbana from the strains derived and grown as described in ref *22*, frozen in liquid nitrogen, and shipped in dry ice to Paris.

Horse heart myoglobin (Mb) was purchased from Sigma and prepared at a concentration of ~100 μM in 100 mM sodium phosphate buffer, pH 7.4. Unliganded Mb was obtained by reduction with sodium dithionite under anaerobic conditions. MbCO was obtained by subsequently exposing the sample to several cycles of CO and vacuum.

Absolute absorption spectra of the samples were recorded with a Shimadzu UV−vis 1601 spectrophotometer. Multicolor femtosecond absorption spectroscopy (*23*) was performed at a repetition rate of 30 Hz, for cytochrome *bd* using the amplified fundamental centered at 620 nm as a pump pulse (70 fs fwhm), and a compressed white light continuum as probe pulse. The polarization of the pump pulse was set parallel, perpendicular, or at magic angle (54.7°) with respect to that of the probe pulse using a sheet polarizer and a half-wave plate. The sample was being continuously moved perpendicular to the beams during the measurements. Scans were recorded with a 4/50 ps dual time base. Femtosecond experiments on CO-myoglobin were performed as described (*24*) with excitation at 563 nm and 50 ps scans. Global exponential fitting of the data in terms of decay-associated spectra was performed with a procedure described previously (*25*) involving singular value decomposition and deconvolution with the instrument response function. The spectra on the 50 ps time scale correspond to the asymptotic value for the R−CO (and MbCO) samples and to the sum of the slowest decaying phase [>70 ps (*14*)] and the asymptotic value for the MV−CO samples.

The photoinduced absorption changes in the membranes were measured with a home-built nanosecond spectrophotometer described in ref *26*. The exciting flash was provided by a Nd:Yag pumped dye laser (640 nm, 5 ns fwhm). The

[1] Abbreviations: MV, mixed valence; R, reduced; Mb, myoglobin; fwhm, full width at half-maximum.

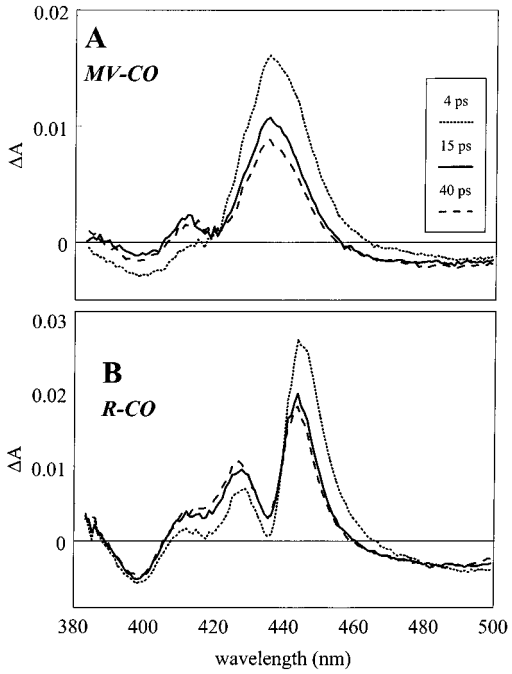

FIGURE 2: Transient absorption spectra measured after photodissociation of CO from the MV−CO (A) and R−CO (B) complexes under isotropic conditions (pump and probe polarized at magic angle).

absorption changes were probed at discrete wavelengths and delay times after the exciting flash by flashes provided by an optical parametric oscillator pumped by the third harmonic of a Nd:Yag (5 ns fwhm).

RESULTS

Steady-State Spectra. The ground-state absorption spectra of the R, R−CO, and MV−CO states of the enzyme (Figure 1) are similar to those published earlier (*21*, *27*, *28*). The strong Soret band is dominated by contributions from the *b*-type hemes. The peak at 430 nm is attributed to heme b_{558} (*29*), and the shoulder at 440 nm has been shown recently to originate from heme b_{595} (*14*). Heme *d* is thought to contribute but weakly to the Soret band (*2*, *30*). The highly unusual difference spectrum associated with CO binding to heme *d* in the fully reduced enzyme (Figure 1, inset) displays many features in the Soret region that presumably originate from steric or electronic interactions of heme *d* with the *b*-type hemes, in particular, heme b_{595} (*14*). We have explored these features to obtain information about the heme−heme and heme−CO interactions.

Isotropic Difference Spectra. For multichromophore systems, direct comparison of the spectra obtained under different conditions on the femtosecond and picosecond time scale requires elimination of any photoselection (polarization) effects. As shown and discussed below, such effects are quite significant for cytochrome *bd* (cf. Figure 5). Therefore, it is essential to obtain isotropic polarization data for cytochrome *bd* at different redox states for a comprehensive analysis. Figure 2 shows transient spectra at different delay times obtained under isotropic conditions (magic angle excitation) following CO photodissociation from reduced heme *d* for the enzyme in the MV−CO and R−CO states. The spectra are generally similar to those reported earlier for parallel excitation (*14*), but the ratio of the peaks are markedly

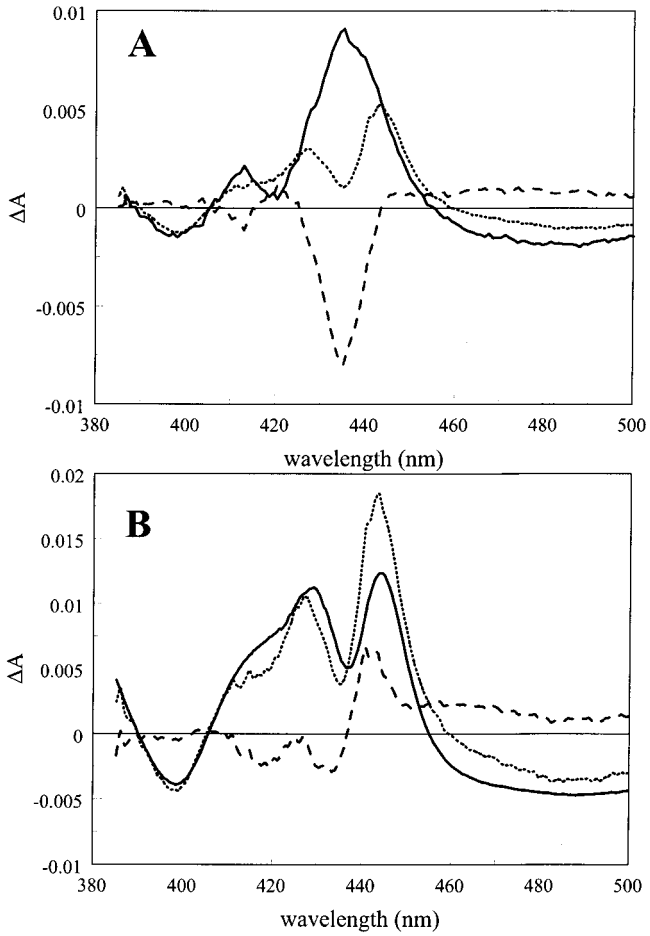

FIGURE 3: (A) Comparison of the isotropic transient absorption spectra on the 50 ps time scale obtained from a global analysis (see text) for the R−CO (dotted) and MV−CO (solid) complexes. The spectra are normalized at 400 nm (spectrum R−CO divided by 3.5). Dashed line: difference between R−CO and MV−CO transient spectra. (B) Comparison of the R−CO isotropic transient absorption spectra on the 50 ps time scale (dotted; same as dotted curve in panel A) and the steady-state unliganded minus CO-liganded spectrum (solid; from inset to Figure 1, inverted). The spectra are normalized on the bleaching feature near 400 nm. Dashed line: difference between the two spectra.

different, in particular, for R−CO (cf. Figure 5 below). In addition, we have now extended the spectral range more to the blue, allowing to fully resolve the bleaching centered at 398 nm present in both forms of the enzyme. At shorter delay times (4 ps) the spectra contain contributions from the excited states as well as the unliganded ground states (*14*). After 15 ps, the R−CO transient spectra correspond to the unliganded ground state minus CO-liganded ground state and do not further change on the time scale of the measurements. In contrast, the corresponding MV−CO spectrum decays significantly on the time scale of tens and hundreds of picoseconds (*14*), presumably reflecting geminate recombination of CO with heme *d*.

Figure 3A compares the ground-state magic angle difference spectra corresponding to the photodissociated MV−CO and R−CO species. The shape of the negative feature around 398 nm is very similar for both species, suggesting that it reflects bleaching of the Soret ground state of heme *d*−CO. Normalization at this band yields spectra that are very similar below 410 nm. With this normalization, the main difference between the R−CO and MV−CO photodissocia-

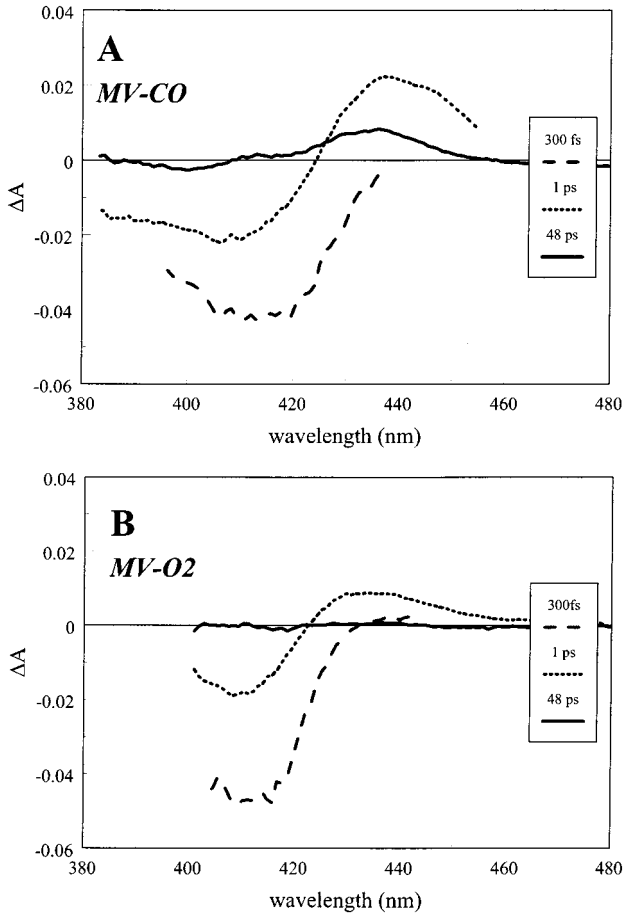

FIGURE 4: Transient absorption spectra measured after photoexcitation of the MV−CO (A) and MV−O_2 (as-prepared) (B) complexes at various delay times. The pump and probe pulses were polarized in parallel.

tion spectra comes out as a bleaching feature centered at 435 nm in the R−CO transient spectrum, which is superimposed on a stronger and broader induced absorption band extending from ~420 to 450 nm. This analysis somewhat deviates from the shift-like difference previously reported (*14*), which did not take into account polarization effects and was restricted to a smaller probe wavelength region (see Discussion).

It should be noted that whereas the *shape* of the bleaching band at 398 nm is similar for MV−CO and R−CO, its *amplitude* (after ~15 ps) is much lower for MV−CO; a normalization factor of 3.5 was used in Figure 3A. As the heme *d* extinction at the excitation wavelength of 620 nm is very similar for both species (Figure 1), this indicates that, in MV−CO, part of the CO photodissociation is "lost" at early times, either because of decreased quantum yield of dissociation from the heme *d* excited state or because of a very fast geminate recombination process.

In principle, discrimination between these possibilities may come from the analysis of the transient spectra at shorter times. Quantitative analysis is difficult, as the early (first few picoseconds) spectra in MV−CO are dominated by the spectral evolution reflecting the photophysics of the ferric *b*-type hemes, which absorb strongly in the probe region around 400 nm and presumably may be photoexcited at 620 nm (Figure 4A). However, we note that, at very early times (1 ps spectrum), the induced absorption at ~435 nm (the maximum of the MV−CO spectrum at longer times) amounts to substantially less than 3.5 times the induced absorption at delay times >15 ps. As in this spectral region excited states of ferric *b*-hemes also are expected to absorb (see below), this strongly indicates that the quantum yield for photodissociation of CO from MV−CO is low.

Figure 3B compares the unpolarized 50 ps and static difference spectra corresponding to CO dissociation from the fully reduced enzyme. The main characteristics of the curves are similar, and the close similarity of the bleaching feature around 400 nm allows for reliable normalization. The main difference between the spectra appears then as a red shift of the bleaching feature near 435 nm mentioned above.

Polarized Spectra. Figure 5 shows the polarized spectra corresponding to the unliganded minus CO-liganded states on the 50 ps time scale after photodissociation, extracted from the data by a global analysis (see Materials and Methods). On this time scale, rotational reorientation of proteins can be neglected, and the polarization effects can be interpreted in terms of photoselection only.

First, we note that, for both states, the polarization $\Delta A_{\parallel}/\Delta A_{\perp}$ varies over the spectrum. This implies that multiple transitions, with different orientations and/or degeneracy properties (see Appendix), contribute to the spectra. This is consistent with our previous conclusion that both heme *d* and heme b_{595} contribute to the difference spectra of CO photodissociation in the Soret region (*14*). For comparison, the polarized picosecond photodissociation spectra of CO from the monoheme protein myoglobin are also shown in Figure 5 (inset). Here, in contrast, the polarization is constant over the entire Soret region. The polarization effect is weak ($\Delta A_{\parallel}/\Delta A_{\perp}$ ~1.16), as expected for pumping and probing planar transitions (eq A9).

In spectral regions where more than one transition contributes, each with a different wavelength dependence, the polarization will vary with wavelength and, moreover, can reach values outside the ranges expected for single transitions due to compensation effects (see Appendix). By contrast, the polarization is expected to be wavelength independent in the regions dominated by contribution of a single transition, as is the case in the wavelength region around 400 nm (note that the polarization $\Delta A_{\parallel}/\Delta A_{\perp}$ is not well-defined near the zero crossing points). This observation and the finding that the spectral (see above) and polarization properties in this range are independent of the oxidation state of the *b*-hemes (they are very similar for R−CO and MV−CO; see above) strongly suggest that the corresponding feature reflects bleaching of a *d*−CO band with a maximum at 398 nm. This conclusion is corroborated by a recently published CO-induced spectrum of a cytochrome *bd* mutant lacking heme b_{595} (*22*). The polarization around 400 nm has a value of ~2. A similar value is found for R−CO on the red side of the zero crossing point (near 410 nm), suggesting that it mainly reflects induced absorption of the same band. The polarization value of 2 is well above the value expected for probing a planar transition (4/3, eq A5, $\varphi = 0°$, and eq A9, $\psi = 0°$) but is consistent with the pump and probe transitions being linear and at an angle of ~30° (eq A3). Thus we conclude that the optical transitions of heme *d* are *not* 2-fold degenerate in the plane of the heme, consistent with the chromophore being formally a chlorin.

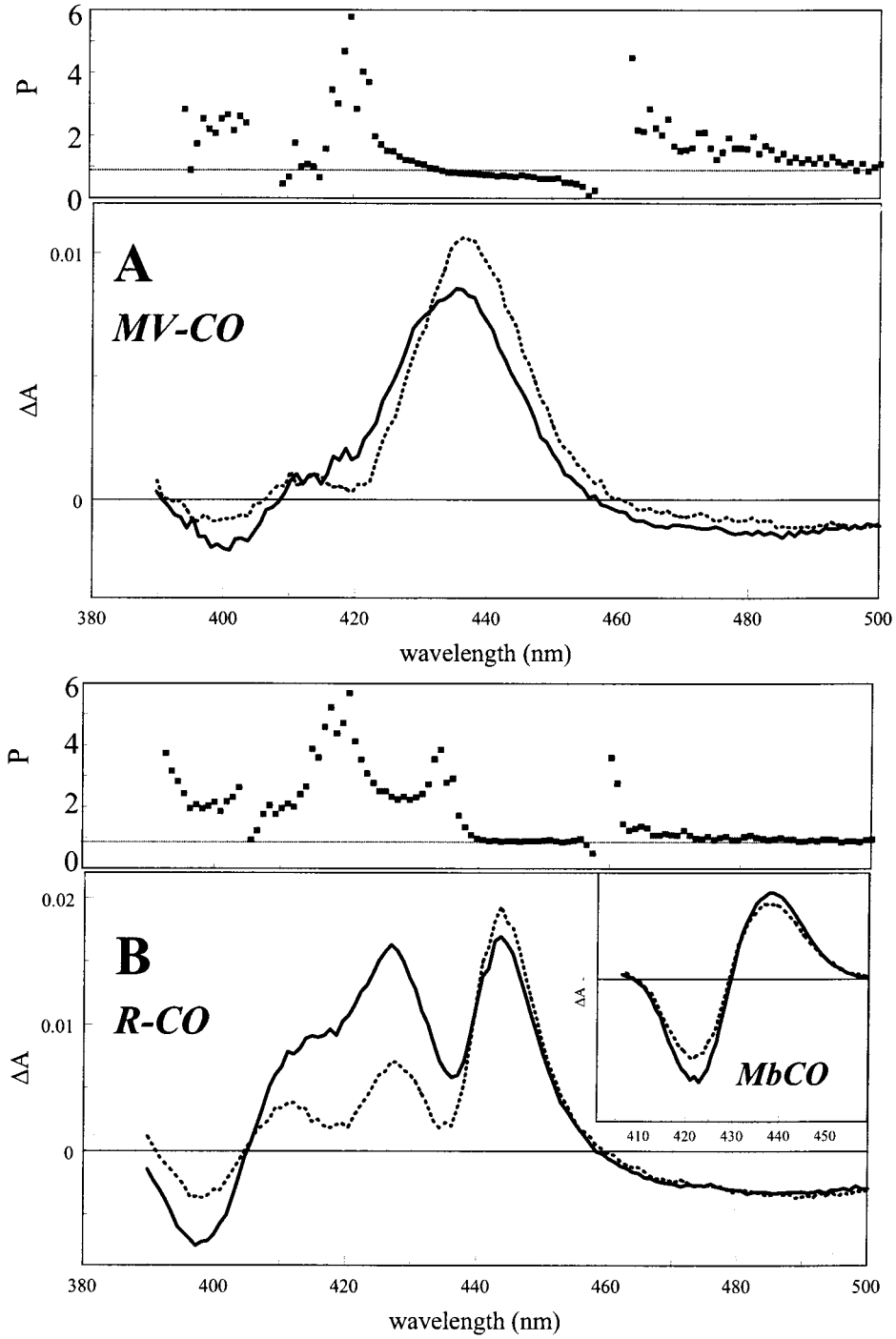

FIGURE 5: Polarized transient absorption spectra on the 50 ps time scale obtained from a global analysis (see text) for the MV−CO (A) and R−CO (B) complexes. The pump and probe pulses were polarized in parallel (solid lines) or perpendicular (dashed lines). The upper panels depict the polarization ratio $P = \Delta A_{\parallel}/\Delta A_{\perp}$ as a function of wavelength. Inset in B: polarized spectra of CO-myoglobin on the 50 ps time scale.

For comparison, in MbCO, which contains a *b*-type heme, the polarization effect is weak ($\Delta A_{\parallel}/\Delta A_{\perp} \sim 1.16$), as expected for pumping and probing planar transitions (eq A9). Here, the polarization is somewhat below the value expected (4/3) for pumping and probing planar transitions in the same plane, possibly indicating a deviation from complete 2-fold degeneracy (cf. ref *31*).

Around 420 nm, a bleaching feature is superimposed on the induced absorption in the spectra of both R−CO and MV−CO forms of cytochrome *bd*, and the total polarization in this region is substantially higher than the maximum value of 3 expected for a single transition. This implies that the polarization associated with the 420 nm bleaching is lower than that of the 398 nm bleaching. The features of the 420 nm bleaching are similar for R−CO and MV−CO. This indicates that it also reflects a bleaching of a *d*−CO band. Altogether, analysis of the blue part of the spectrum indicates the presence of two differently polarized transitions attributable to *d*−CO.

Around 434 nm, a sharp increase in the polarization is observed in R−CO, corresponding to at least part of the dip in the transient spectra (see below). This polarization change,

as well as the dip, are not observed in MV−CO, showing that the feature is not directly associated with reduced heme *d*, consistent with our earlier interpretation that it reflects an absorption change of reduced heme b_{595} in R−CO (*14*) and also indicating that it is not due to an absorption change due to reduction of heme b_{595} in MV−CO (see below). We note that the polarization at both sides of the sharp change, i.e., below 430 nm and, in particular, above 440 nm, is rather flat. This is in agreement with the comparison of the normalized magic angle spectra (Figure 3A), indicating that the feature should be interpreted as a bleaching superimposed on an induced absorption, rather than a shift. Thus, this finding also a posteriori justifies the used normalization (in view of the interactions between hemes *d* and b_{595} the validity of this normalization is nontrivial).

The above-mentioned *increase* in the polarization around 434 nm in R−CO corresponding to the superposition of the sharp *negative* absorption on the broader positive absorption implies that the polarization associated with the bleaching itself is smaller than that of the surrounding induced absorption; i.e., less than 1. Thus, assuming it originates from probing a planar transition (heme b_{595}) upon excitation of a linear transition (heme *d*), the angle between the two hemes should be more than 35° (eq A5).

For R−CO, the polarization is essentially constant (value close to 1.0) at $\lambda > 440$ nm, indicating that this feature originates from a single transition. In this spectral region, the *shape* of the spectrum is similar (but not identical, see below) to R−CO and MV−CO (Figure 3A), suggesting that it corresponds directly to unliganded heme *d*. An attractive possibility is that it corresponds to the same transition as the bleaching around 420 nm, also observed in both species, and which indeed should correspond to a polarization less than 2 (see above).

Assuming that the heme *d* transition pumped at 620 nm is a nondegenerate, linear transition (see above), the polarization ratio of 1.0 will correspond either to an angle of ∼55° between the linear pump transition and a linear probed transition (eq A3) or, alternatively, to an angle of ∼35° between the linear pump transition and a degenerate, planar transition of the probed heme (eq A5). However, in the latter case, if both the pump and the probe transitions originate from the same heme as inferred above, the pump transition should lie in the plane of the probe transition (angle 0°), corresponding to a polarization of 4/3 (eq A5), i.e., higher than the observed polarization (Figure 5B). Therefore, it is most likely that the probed transition can be considered as linear.

Unlike the case of R−CO, the polarization varies gradually above 440 nm in the case of MV−CO (Figure 5A), indicating that more than one transition contributes to the transient spectra in this region. One possibility is that this contribution is due to a small spectral change in the tail of the absorption of one of the (ferric) *b*-type hemes upon CO dissociation from heme *d*, most likely of b_{595}, that is known to respond to photodissociation of the heme *d*−CO complex in the fully reduced state of the enzyme (*14*).

One might suggest that partial electron dislocation from heme *d* to heme b_{595} upon dissociation of CO from heme *d* in the MV−CO state ("backflow of electrons"; e.g., ref *16*) could also contribute to the induced absorption in this wavelength range. Indeed, if the two hemes are within a few angstroms from each other, interheme redox reequilibration on a picosecond time scale cannot be excluded. However, for the following reasons this can hardly be the major reason for the induced band at 435 nm. First, as indicated above, one would then expect sharp, not gradual, polarization changes around 435 nm, which is not observed. Second, the difference in midpoint potentials between the hemes *d* and b_{595} (>100 mV; *2*) suggests that such electron transfer, if appearing at all on the picosecond time scale, could amount to reduction of b_{595} by at most 2−3% (corresponding to an estimated ΔA of less than 10−15% of that observed at 435 nm). Third, the position and line shape of the induced absorption at 434−435 nm in the MV−CO complex do not match satisfactorily those of the reduced b_{595} heme with the Soret maximum at 438−440 nm (cf. refs *14* and *22*, and see Discussion).

Comparison CO- and O_2-Bound Complexes. Figure 4A shows selected transient absorption spectra obtained after excitation of the MV−CO complex, including those at very short delay times, when heme-excited states contribute to the spectra as well. The initial bleaching roughly corresponds to the ground-state absorption, which is dominated by the *b*-type hemes, and the excited state decay of these hemes dominates the spectral evolution on the time scale of a few picoseconds, as stated above. The CO dissociation spectrum appears clearly only after decay of these excited states (the 48 ps spectrum).

Due to high affinity of the ferrous heme *d* for O_2, the "as-prepared" form of cytochrome *bd* is predominantly in the MV−O_2 state. Therefore, it is possible to test if O_2 can be photodissociated. Figure 4B shows that, in contrast to MV−CO, no spectral changes can be observed after decay of the excited states (the 48 ps spectrum). Thus, either O_2 cannot be photodissociated from heme *d* or it recombines within a few picoseconds. To address this issue, a comparison of the transient spectra at 1 ps in the two cases is useful. For MV−O_2, the induced absorption in this spectrum is relatively low compared to MV−CO, and the difference between the two spectra when normalized at the bleaching at ∼410 nm corresponds roughly to the MV−CO difference spectrum at longer delays. This indicates that the MV−O_2 spectrum at ∼1 ps is dominated by contributions from the *b*-type hemes (indeed, the spectrum is very similar to that observed in oxidized cytochrome b_{559} from spinach; M. H. Vos and U. Liebl, unpublished results) and that O_2 dissociation does not contribute to the absorption changes even at 1 ps after excitation. Altogether, we conclude that O_2 cannot be photodissociated at any measurable yield from heme *d* using 620 nm light, at least on the time scale of 1 ps. Also, measurements in the far-red spectral region (>640 nm) where the Q_Y band of the heme *d*−oxy complex contributes significantly do not display spectral changes after decay of the excited states (not shown). Finally, we found no evidence for O_2 dissociation using 310 nm excitation, indicating that the relatively low photon energy in the case of 620 nm excitation cannot explain the remarkable photostability of the *d*−O_2 complex.

Nanosecond Spectroscopy of CO Photodissociation from Membrane-Bound Wild-Type Cytochrome bd and the E445A Mutant Lacking Heme b_{595}. Figure 6 shows transient spectra at 5 ns of the R−CO forms of cytochrome *bd* in membranes from WT (panel B) and the mutant strain carrying E445A

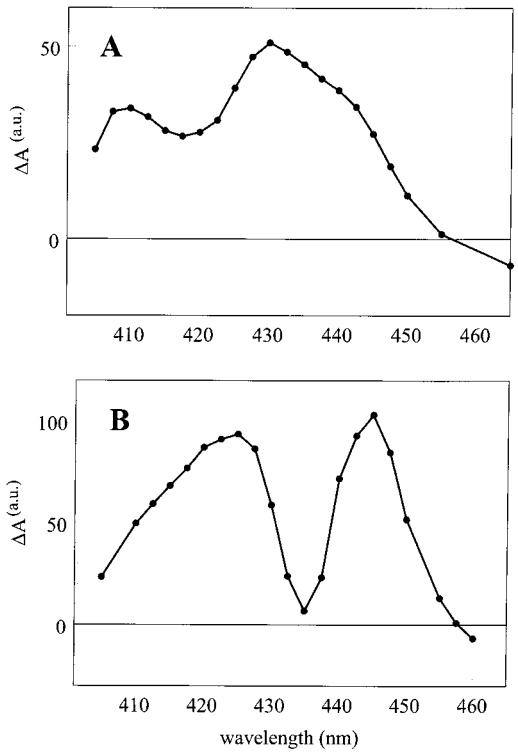

FIGURE 6: Transient spectra of membranes containing E445A mutant (A) and wild-type (B) enzymes at a delay time of 5 ns.

replacement in subunit I of the enzyme (panel A); the mutant expresses cytochrome *bd* mostly devoid of heme b_{595} (*22*). Notably, the line shape of the R−CO mutant photodissociation spectrum is reminiscent of the picosecond transient spectra observed for the WT enzyme in the MV−CO state (*14*; Figure 2A). In particular, it does not display the sharp bleaching feature at 435 nm observed for the R−CO form of the WT membranes under the same experimental conditions (Figure 6B), as well as in the purified enzyme on the picosecond time scale (*14*; Figure 2B). These results further substantiate assignment of the bleaching at 435 nm to heme b_{595} interaction with heme *d* (see above and Discussion). Notably, even after 5 ns, the bleaching seen in the WT R−CO transient spectrum (Figure 6B) and clearly resolved in the corresponding difference spectrum (WT *minus* mutant; not shown) is still at 435 nm, as the WT R−CO picosecond difference spectrum and unlike the static difference spectrum where it shifts to ca. 438 nm (cf. Figure 3). This may indicate that, after 5 ns, the photodissociated CO has not yet left the vicinity of the active site (see Discussion). Full analysis of the nanosecond spectroscopic studies of CO photodissociation from membrane-bound WT and mutant cytochrome *bd* in different redox states will be published elsewhere.

DISCUSSION

Quinol oxidase *bd* is a three-heme-containing heterodimer, and there are interactions between at least two of the hemes (heme *d* and heme b_{595}) such that perturbation of one heme influences the other heme within picoseconds. This latter feature, to the best of our knowledge unique for heme proteins, implies that photoselection effects are likely to play a role in the spectroscopy of the electronic transitions of cytochrome *bd* (*14*). Indeed, such effects have been observed in this work, and we have exploited them to elicit the spectroscopic properties and interaction between hemes *d* and b_{595} in more detail than was possible in a previous work (*14*), performed under parallel excitation conditions only. Interestingly, this is the first instance of studying photoselection effects in UV/vis transient absorption experiments of heme proteins, including the classical "model" systems such as myoglobin, presumably because such effects are not too informative for monoheme mechanisms [photoselection effects have been exploited in transient infrared spectroscopy, where they can yield structural information (*32*, *33*)].

In particular, we have now assessed that in cytochrome *bd* the unusual W-shape of the R−CO *minus* R spectrum in the Soret region can be attributed to a superimposition of a strong induced absorption at 435 nm, presumably due to an electronic perturbation of heme b_{595} upon CO binding to heme *d*. In addition, the difference between the static CO-induced difference spectrum and the one observed on the picosecond time scale under anisotropic polarization conditions can be described merely as a small red shift of the heme b_{595} Soret band. This is at variance with our previous analysis that did not take into account polarization effects (*14*), and it is now clear that transient binding of CO to heme b_{595} need not be invoked to explain the spectrum. The difference between the 50 ps and static CO-photodissociation spectra of the fully reduced cytochrome may be due to the initial "caging" of the dissociated CO near heme b_{595}. The studies on the membrane-bound *bd* with a longer observation time window indicate that this caging of CO persists for at least 5 ns.

The polarized spectra yield detailed information on the position of the electronic bands of heme *d* in the Soret region. Two transitions in the Soret regions were identified as *d*−CO transitions, at ∼398 nm and at ∼420 nm, with transition moments oriented at respectively ∼30° and ∼55° with respect to the Q-band transition at 634 nm. The most likely positions for the corresponding unliganded *d* transitions are at 410 and ∼440 nm (broader). The observation of two separate, nondegenerate, transitions is consistent with the nonsymmetry of the macrocycle of heme *d* (*34*−*36*) and with the CO-induced difference spectrum of the cytochrome *bd* mutant containing no heme b_{595} (cf. Figure 5 in ref *22*). We note that a split Soret band was also observed in a CO-ligated octo-ethyl chlorin and other six-coordinated low-spin ferrous chlorines (*37*).

The most striking difference between the R−CO and MV−CO time-resolved photodissociation spectra as compared under both magic angle (Figure 3A) and polarization conditions (Figure 5) is the bleaching around 434 nm. At selective excitation of heme *d*, this bleaching is absent in the transient spectra of the (WT) MV−CO state as well as in the R−CO state of the E445A mutant lacking heme b_{595} (Figure 6). Accordingly, the band is missing in the static (R−CO *minus* R) difference spectrum of the E445A mutant (*22*). These results point out a fast reduction of the oscillator strength of a reduced heme b_{595} absorption band upon CO dissociation from heme *d* as the origin of this bleaching. The band appears to shift a few nanometers to the red after CO leaves the protein (cf. the picosecond and static spectra in Figure 3B). Both the magic angle spectra and the polarization data indicate no substantial contribution from this feature above 440 nm. Thus, the bleaching feature is somewhat blue shifted relative to the maximum of the Soret absorption

spectrum of heme b_{595} deduced previously (*14*) from the recovery of the initial bleaching observed upon excitation of the fully reduced enzyme at 590 nm (near the maximum of the Q absorption band of heme b_{595}) and confirmed by subsequent studies of the b_{595}-deficient mutant of cytochrome *bd* (*22*). Possible explanations for this difference may include (a) a slight splitting of the Soret absorption of heme b_{595} dissociation of CO from heme *d* having a stronger effect on the higher energy component (B_x) of the overall Soret band of b_{595} and (b) excitonic interactions (see below). The angle between the (presumably linear) heme *d* transition at 634 nm and the (presumably planar) heme b_{595} Soret transition is assessed at >35°, consistent with EPR data that yielded an angle of 55° between the two heme planes (*38*). As we discussed previously (*14*), the origin of the perturbation of the heme b_{595} spectrum upon dissociation of CO from heme *d* is likely to be due to an alteration in steric or excitonic interaction between the two, presumably close-lying, cofactors. Recent circular dichroism studies of Arutjunjan et al. (paper in preparation) do indeed indicate considerable electronic interactions between hemes *d* and b_{595} under static conditions. In an exciton-coupled system, transitions are admixtures of contributions from different chromophores, and such effects might further contribute to variability of the "heme b_{595} band" discussed above.

Photodissociation Yield of CO and O_2. A novel observation is that the photodissociation yield of CO from heme *d* is much less for MV−CO than for R−CO. Assuming a quantum yield of photodissociation of 1 for R−CO, our present results indicate that in MV−CO only ∼30% of CO does dissociate upon absorption of a photon by heme *d*. Our previous results have shown that about half of the 30% dissociated CO recombines within a few hundred of picoseconds (*14*). Thus, interactions between hemes b_{595} and *d* influence both the photostability of CO complex and, once dissociated, the further fate of the ligand. It was previously discussed that dependence of photodissociated CO dynamics on the redox state of heme b_{595} suggests a role of the latter heme b_{595} in controlling the ligand traffic to and from heme *d* (*14*); our present results indicate that this scenario does not necessarily invoke transient binding of CO to heme b_{595}.

Intriguing, and possibly physiologically relevant, is the finding that the quantum yield of O_2 dissociation is zero for the mixed-valence complex. This finding is generally consistent with the high affinity of the enzyme for O_2 (*39*); yet the nonphotodissociability of O−O (or any other diatomic, atomic oxygen containing, ligand) is thus far unprecedented for heme proteins (*40*). Such a strong decrease in the yield of photodissociation implies that the electronic state reached by excitation of MV−O_2 with a 620 nm (or higher energy) photon does not lead to a dissociative channel and that the electronic configuration is altered with respect to CO as a ligand. The ensemble of results (dissociation yield decreases in the sequence R−CO > MV−CO > MV−O_2) thus may suggest that the high affinity of the enzyme for O_2 is due to the specific properties of the chlorin-containing binding site and that, in particular, the interaction between hemes *d* and b_{595} plays an important role.

APPENDIX

In transient absorption experiments, photoselection effects can result in differences in the signals with the probe pulse polarized parallel ($\Delta A_{\parallel}$) and perpendicular ($\Delta A_{\perp}$) to the pump beam. This difference depends on the angle θ between the unit transition moments μ_e and μ_p of the excited and the probed transition, respectively. The anisotropy, *r*, is defined as

$$r = \frac{\Delta A_{\parallel} - \Delta A_{\perp}}{\Delta A_{\parallel} + 2\Delta A_{\perp}} \tag{A1}$$

For linear transitions (*41*)

$$r = \frac{3\cos^2\theta - 1}{5} \tag{A2}$$

which gives, with (A1), values for the polarization between 1/2 and 3:

$$\frac{\Delta A_{\parallel}}{\Delta A_{\perp}} = \frac{1 + 2\cos^2\theta}{2 - \cos^2\theta} \tag{A3}$$

For 2-fold degenerate transitions (planar transitions), such as those in isolated *b*-type hemes, the anisotropy effects are less strong. The case of excitation in a degenerate transition and probing a linear transition has been treated by Moore et al. (*32*):

$$r = \frac{3\cos^2\varphi - 2}{10} \tag{A4}$$

Here φ is the angle between the linear transition and the plane. Using (A1) this results in polarization values between 1/2 and 4/3:

$$\frac{\Delta A_{\parallel}}{\Delta A_{\perp}} = \frac{2 + 2\cos^2\varphi}{4 - \cos^2\varphi} \tag{A5}$$

To our knowledge, an expression for the polarization effects of excitation and probing 2-fold degenerate transitions making an angle ψ has not yet been derived. Extending the method used in ref *32*, we calculate the anisotropy from the average of the anisotropies r_x and r_y corresponding to the axis in the plane of the probed chromophore making an angle ψ with the plane of the excited chromophore (*x*) and the common axis of both planes (*y*):

$$r_x = \frac{3\cos^2\psi - 2}{10} \tag{A6}$$

$$r_y = \frac{1}{10} \tag{A7}$$

$$r = \frac{r_x + r_y}{2} = \frac{3\cos^2\psi - 1}{20} \tag{A8}$$

Using (A1), we find polarization values comprised between the interval 6/7 to 4/3:

$$\frac{\Delta A_{\parallel}}{\Delta A_{\perp}} = \frac{6 + 2\cos^2\psi}{7 - \cos^2\psi} \tag{A9}$$

We stress that, for all cases, the polarization values assume that one probes only one transition. The situation for overlapping bands with inverted signs (i.e., induced absorp-

tion and bleaching) can lead to a wider range of polarizations, in principle ranging from $-\infty$ to ∞.

ACKNOWLEDGMENT

We are indebted to Dr. I. F. Bukhova for growing the cells and to Drs. A. M. Arutjunjan and P. Joliot for useful discussions.

REFERENCES

1. Henry, M. F. (1981) in *Cyanide in Biology* (Vennesland, B., Conn, E. E., Knowles, C. J., Westley, J., and Wissing, F., Eds.) pp 415−436, Academic Press, London.
2. Junemann, S. (1997) *Biochim. Biophys. Acta 1321*, 107−127.
3. Tsubaki, M., Hori, H., and Mogi, T. (2000) *J. Inorg. Biochem. 82*, 19−25.
4. Poole, R. K., and Cook, G. M. (2000) *Adv. Microb. Physiol. 43*, 165−224.
5. Endley, S., McMurray, D., and Ficht, T. A. (2001) *J. Bacteriol. 183*, 2454−2462.
6. Way, S. S., Sallustio, S., Magliozzo, R. S., and Goldberg, M. B. (1999) *J. Bacteriol. 181*, 1229−1237.
7. Zhang-Barber, L., Turner, A. K., Martin, G., Frankel, G., Dougan, G., and Barrow, P. A. (1997) *J. Bacteriol. 179*, 7186−7190.
8. Osborne, J. P., and Gennis, R. B. (1999) *Biochim. Biophys. Acta 1410*, 32−50.
9. Ferguson-Miller, S., and Babcock, G. T. (1996) *Chem. Rev. 7*, 2889−2907.
10. Rothery, R. A., Houston, A. M., and Ingledew, W. J. (1987) *J. Gen. Microbiol. 133*, 3247−3255.
11. Krasnoselskaya, I., Arutjunjan, A. M., Smirnova, I., Gennis, R. B., and Konstantinov, A. A. (1993) *FEBS Lett. 327*, 279−283.
12. Hill, J. J., Alben, J. O., and Gennis, R. B. (1993) *Proc. Natl. Acad. Sci. U.S.A. 90*, 5863−5867.
13. Tsubaki, M., Hori, H., Mogi, T., and Anraku, Y. (1995) *J. Biol. Chem. 270*, 28565−28569.
14. Vos, M. H., Borisov, V. B., Liebl, U., Martin, J.-L., and Konstantinov, A. A. (2000) *Proc. Natl. Acad. Sci. U.S.A. 97*, 1554−1559.
15. Puustinen, A., Finel, M., Haltia, T., Gennis, R. B., and Wikström, M. (1991) *Biochemistry 30*, 3936−3942.
16. Jasaitis, A., Borisov, V. B., Belevich, N. P., Morgan, J. E., Konstantinov, A. A., and Verkhovsky, M. I. (2000) *Biochemistry 39*, 13800−13809.
17. Ostermeier, C., Harrenga, A., Ermler, U., and Michel, H. (1997) *Proc. Natl. Acad. Sci. U.S.A. 94*, 10547−10553.
18. Yoshikawa, S., Shinzawa-Itoh, K., Nakashima, R., Yaono, R., Inoue, N., Yao, M., Fei, M. J., Libeu, C. P., Mizushima, T., Yamaguchi, H., Tomizaki, T., and Tsukihara, T. (1998) *Science 280*, 1723−1729.
19. Soulimane, T., Buse, G., Bourenkov, G. B., Bartunik, H. D., Huber, R., and Than, M. E. (2000) *EMBO J. 19*, 1766−1776.
20. Borisov, V. B., Arutyunyan, A. M., Osborne, J. P., Gennis, R. B., and Konstantinov, A. A. (1999) *Biochemistry 38*, 740−750.
21. Borisov, V. B., Selednikova, S. E., Poole, R. E., and Konstantinov, A. A. (2001) *J. Biol. Chem. 276*, 22095−22099.
22. Zhang, J., Hellwig, P., Osborne, J. P., Huang, H.-w., Moenne-Loccoz, P., Konstantinov, A. A., and Gennis, R. B. (2001) *Biochemistry 40*, 8548−8556.
23. Martin, J.-L., and Vos, M. H. (1994) *Methods Enzymol. 232*, 416−430.
24. Vos, M. H., Lambry, J.-C., and Martin, J.-L. (2000) *J. Chin. Chem. Soc. 47*, 765−768.
25. Liebl, U., Lambry, J.-C., Leibl, W., Breton, J., Martin, J.-L., and Vos, M. H. (1996) *Biochemistry 35*, 9925−9934.
26. Béal, D., Rappaport, F., and Joliot, P. (1999) *Rev. Sci. Instrum. 70*, 202−207.
27. Miller, M. J., and Gennis, R. B. (1983) *J. Biol. Chem. 258*, 9159−9165.
28. Junemann, S., and Wrigglesworth, J. M. (1995) *J. Biol. Chem. 270*, 16213−16220.
29. Poole, R. K. (1988) in *Bacterial Energy Transduction* (Anthony, C., Ed.) pp 231−291, Academic Press, London.
30. Hori, H., Tsubaki, M., Mogi, T., and Anraku, Y. (1996) *J. Biol. Chem. 271*, 9254−9258.
31. Eaton, W. A., and Hofrichter, J. (1976) *Methods Enzymol. 76*, 175−261.
32. Moore, J. N., Hansen, P. A., and Hochstrasser, R. M. (1988) *Proc. Natl. Acad. Sci. U.S.A. 85*, 5062−5066.
33. Lim, M., Jackson, T. A., and Anfinrud, P. A. (1997) *Nat. Struct. Biol. 4*, 209−214.
34. Chang, V., Morell, D. B., Nichol, A. W., and Clezy, P. S. (1970) *Biochim. Biophys. Acta 215*, 88−96.
35. Martinis, S. A., Sotiriou, C., Chang, C. K., and Sligar, S. G. (1989) *Biochemistry 28*, 879−884.
36. Bracete, A. M., Kadkhodayan, S., Sono, M., Huff, A. M., Zhuang, C., Cooper, D. K., Smith, K. S., Chang, C. K., and Dawson, J. H. (1994) *Inorg. Chem. 33*, 5042−5049.
37. Sono, M., Bracete, A. M., Huff, A. M., Ikeda-Saito, M., and Dawson, J. H. (1991) *Proc. Natl. Acad. Sci. U.S.A. 88*, 11148−11152.
38. Ingledew, W. J., Rothery, R. A., Gennis, R. B., and Salerno, J. C. (1992) *Biochem. J. 282*, 255−259.
39. Hill, B. C., Hill, J. J., and Gennis, R. B. (1994) *Biochemistry 33*, 15110−15115.
40. Vos, M. H., and Martin, J.-L. (1999) *Biochim. Biophys. Acta 1411*, 1−20.
41. Van Amerongen, H., and Struve, W. S. (1995) *Methods Enzymol. 246*, 259−283.

BI0158019